A novel strategy for surface modification of superparamagnetic iron oxide nanoparticles for lung cancer imaging†

Gang Huang,[a] Chunfu Zhang,[ab] Shunzi Li,[ac] Chalermchai Khemtong,[a] Su-Geun Yang,[a] Ruhai Tian,[a] John D. Minna,[ad] Kathlynn C. Brown[ac] and Jinming Gao*[a]

Received 9th February 2009, Accepted 24th April 2009
First published as an Advance Article on the web 29th May 2009
DOI: 10.1039/b902358e

Superparamagnetic iron oxide (SPIO) nanoparticles are widely used in magnetic resonance imaging (MRI) as versatile ultra-sensitive nanoprobes for cellular and molecular imaging of cancer. In this study, we report a one-step procedure for the surface functionalization of SPIO nanoparticles with a lung cancer-targeting peptide. The hydrophobic surfactants on the as-synthesized SPIO are displaced by the peptide containing a poly(ethylene glycol)-tethered cysteine residue through ligand exchange. The resulting SPIO particles are biocompatible and demonstrate high T_2 relaxivity. The nanoprobes are specific in targeting $\alpha_v\beta_6$–expressing lung cancer cells as demonstrated by MR imaging and Prussian blue staining. This facile surface chemistry and the functional design of the proposed SPIO system may provide a powerful nanoplatform for the molecular diagnosis of lung cancer.

Introduction

Lung cancer is the most common cause of cancer-related death worldwide, with 1.4 million deaths occurring annually.[1] It is also the leading cause of cancer death in the US, expected to account for 31% and 26% mortality in men and women in 2008, respectively.[2] Development of advanced imaging probes that provide information at the molecular and cellular levels is crucial for the molecular diagnosis and targeted therapy of lung cancer. Recently, superparamagnetic nanoparticles (*e.g.*, Fe_3O_4,[3–5] $MnFe_2O_4$[6]) have received considerable attention as molecular imaging probes with substantially higher molar relaxivities over small molecular T_1 agents (*e.g.*, Gd-DTPA). Considerable effort has been devoted to strategies to increase the cancer specificity of superparamagnetic probes to target unique molecular markers of solid tumors.[7–10] Surface functionalization of the superparamagnetic iron oxide (SPIO) nanoparticles has provided multiple examples of targeted contrast agents that specifically recognize tumor markers such as transferrin receptor,[11] folate receptor,[12] and Her-2/neu.[6,13] Despite these successes, the current modification strategies may suffer from several limitations. For example, although coating of SPIO nanoparticles with a silica[14] or gold[15] shell can greatly facilitate ligand attachment, the added layer may compromise the efficiency of SPIO in relaxing the surrounding water molecules. On the other hand, most currrent surface functionalization procedures require several synthetic steps with reactive intermediates, which makes it inconvenient for the wide use of SPIO in cancer molecular imaging applications.

In this study, we report a one-step method to functionalize the surface of SPIO particles with a lung cancer-targeting peptide

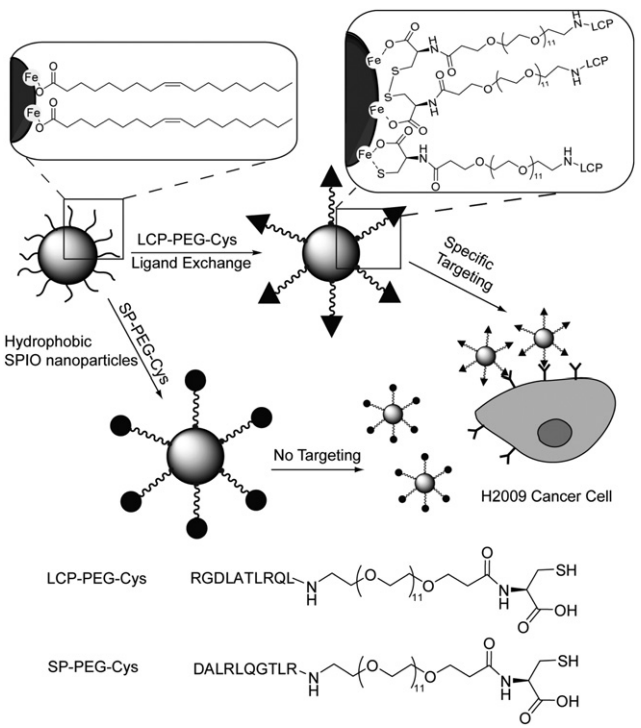

Scheme 1 Surface modification of superparamagnetic iron oxide (SPIO) nanoparticles with LCP-PEG-Cys for lung cancer targeting. A scrambled peptide control (SP-PEG-Cys) is included to examine the $\alpha_v\beta_6$ specificity for cell targeting.

[a]*Department of Pharmacology, Harold C. Simmons Comprehensive Cancer Center, 5323 Harry Hines Blvd, Dallas, Texas, 75390, USA. E-mail: jinming.gao@utsouthwestern.edu; Fax: +1 214 645 6347; Tel: +1 214 645 6370*
[b]*Med-X Research Institute, Shanghai Jiaotong University, Shanghai, China*
[c]*Department of Internal Medicine, Division of Translational Research, 5323 Harry Hines Blvd, Dallas, Texas, 75390, USA; Fax: +1 214 645 6347; Tel: +1 214 645 6370*
[d]*Hamon Center for Therapeutic Oncology, UT Southwestern Medical Center at Dallas, 5323 Harry Hines Blvd, Dallas, Texas, 75390, USA; Fax: +1 214 645 6347; Tel: +1 214 645 6370*

† This paper is part of a *Journal of Materials Chemistry* theme issue on inorganic nanoparticles for biological sensing, imaging, and therapeutics. Guest editor: Jinwoo Cheon.

(LCP, Scheme 1). The peptide, named H2009.1 (RGDLATLRQL), was isolated from a phage-displayed peptide library by biopanning on the lung adenocarcinoma cell line H2009.[16,17] This peptide binds to the restrictively expressed integrin, $\alpha_v\beta_6$, which is up-regulated in many human non-small cell lung carcinomas compared with normal lung tissue.[18] In order to incorporate this peptide onto the SPIO surface, the peptide was synthesized with a poly(ethylene glycol) (PEG_{11}) linker followed by a cysteine residue at the C-terminus of the peptide (NH_2-RGDLATLRQL-PEG_{11}-Cys-COOH, or LCP-PEG-Cys). Here we demonstrate the peptide was able to replace the hydrophobic surfactants on the as-synthesized SPIO nanoparticles through direct ligand exchange. The resulting nanoparticles have shown specific targeting to the $\alpha_v\beta_6$–postive H2009 cells over $\alpha_v\beta_6$–negative H460 cells as well as over a scrambled peptide (SP, with the sequence of DALRLQGTLR-PEG_{11}-Cys-COOH, or SP-PEG-Cys)-SPIO control. The facile surface chemistry and ability to incorporate the SPIO chelator as part of solid phase peptide synthesis have the potential to greatly facilitate the use of SPIO for molecular imaging applications.

Experimental

Materials

Fmoc-amino polyethylene glycol propionic acid ($C_{42}H_{65}NO_{16}$, Fmoc-NH-$(PEG)_{11}$-COOH) was purchased from Polypure, Oslo, Norway. Fmoc-Cys(Trt)-Wang resin (substitution level 0.59 mmol/g) and all other amino acids were obtained from EMD Biosciences Inc. Dimethylformamide (DMF) and trifluoroacetic acid (TFA) were purchased from Applied biosystems Inc. O-Benzotriazole-*N*,*N*,*N*′,*N*′-tetramethyl-uronium-hexafluoro-phosphate (HBTU) and N-hydroxybenzotriazole (HOBt) were obtained from Novabiochem. All the other reagents were purchased from Sigma-Aldrich.

Synthesis of superparamagnetic iron oxide particles

Oleic acid-coated hydrophobic SPIO nanoparticles were prepared by thermal decomposition of ferric acetylacetonate ($Fe(acac)_3$) according to a previously published procedure.[19] Briefly, $Fe(acac)_3$ (1 mmol), oleic acid (3 mmol), oleylamine (3 mmol) and 1,2-hexadecanediol (5 mmol) were dissolved in 10 mL phenyl ether. The mixture was heated under nitrogen environment at 200 °C for 2 h before refluxing the solution at 300 °C for another 1 h. SPIO particles were precipitated with 20 mL ethanol and resuspended in 10 mL hexane. Uniform SPIO particles (6.2 ± 0.9 nm in diameter) were obtained by sequential centrifugations and ethanol precipitations. The size of these hydrophobic SPIO particles were determined by transmission electron microscopy (TEM, JEOL 1200EX II, JOEL USA, Inc., Peabody, MA) and calculated by averaging the size of 300 particles measured by Image J software.

Syntheses of LCP-PEG-Cys and SP-PEG-Cys peptides

Peptide syntheses were carried out on a Symphony™ Synthesizer (Rainin Instruments, Protein Technologies, Inc. Woburn, MA) by Fmoc solid phase peptide synthesis using Fmoc-Cys(Trt)-Wang resin. Fmoc-protected amino acids were coupled at a 5-fold excess using HBTU, HOBt and *N*-methylmorpholine (NMM) for coupling (45 min). 20% piperidine in DMF was used to remove N-terminal Fmoc protecting groups. Fmoc-NH-$(PEG)_{11}$-COOH was coupled in the same fashion. Upon completion of the synthesis, peptides were cleaved from the resin using a TFA : 1,2-ethanedithiol (EDT) : H_2O : triisopropylsilane cocktail (94 : 2.5 : 2.5 : 1) and precipitated in cold diethyl ether. Crude peptides were purified by reverse phase HPLC using an Aapptec Spirit peptide C18 column (250 mm × 21.2 mm, 5 μm). The purified peptides were analyzed by analytical RP-HPLC (Varian, RP-C18 column, 250mm × 4.6mm, 5 μm) and were greater than 95% purity. The peptide molecular weights were confirmed by MALDI-MS (Voyager DE™ Pro instrument, Applied Biosystems Inc, Carlsbad, CA, USA).

Surface modification of SPIO nanoparticles

In a typical procedure, SPIO nanoparticles (2.0 mg) were dispersed in 200 μL toluene and mixed with LCP/SP-PEG-Cys (2.0 mg) dissolved in dimethylsulfoxide (DMSO) (200 μL). The mixture was kept at 60 °C for 2 h under nitrogen environment. After cooling to room temperature, the peptide-coated SPIO was precipitated with a mixture of ethanol, chloroform and hexane (1 : 1 : 2) and redispersed in water. The size and morphology of the peptide-coated SPIO particles were characterized with transmission electron microscopy and dynamic light scattering (DLS 802, Viscotek, Houston, TX, USA). Peptide quantities binding on the surface of SPIO particles were analyzed by the W.M. Keck Facility, Yale University. The magnetic properties of peptide and oleic acid coated particles were measured from the hysteresis curves of air-dried SPIO particles by using an alternate gradient magnetometer (AGM, MicroMag 2900, Princeton Measurements, NJ, USA). The T_2 relaxation times were measured by a 0.47 T relaxometer (Maran Ultra, UK) with standard Carr-Purcell-Meiboom-Gill (CPMG) sequence and inversion-recovery technique.

Cell uptake and viability studies

Human lung cancer cell lines, $\alpha_v\beta_6$–postive H2009 cells and $\alpha_v\beta_6$–negative H460 cells, were used for all the *in vitro* biological studies.[20] The cells were maintained in an RPMI culture medium supplemented with 5% fetal bovine serum and 1% penicillin and streptomycin (37 °C, 5% CO_2). For cell uptake studies, H2009 and H460 cells were plated in 8-well chamber slides (Poly-D-Lysine Cellware CultureSlide, BD Bioscience, Bedford, MA, USA) and incubated with culture medium containing LCP-SPIO or SP-SPIO at Fe concentrations of 0.03 mM for 0.5 and 2 h. After incubation, the media was removed and cells were washed with PBS three times. Subsequently, cells were fixed with methanol for 5 min and acetone for 1 min at −20 °C. For staining, the fixed cells were incubated with 10% Prussian blue for 5 min and then a mixture of 10% Prussian blue and 20% hydrochloride acid (v/v, 1 : 1) for 30 min. The cells were counter stained with nuclear fast red for 5 min. Images were acquired with a Leica fluorescent microscope (Leica DM5500 B, Chicago, IL, USA).

For viability studies, H2009 and H460 cells were incubated at different Fe concentrations (0.03 or 0.3 mM) of LCP-SPIO or SP-SPIO for 24 h. The cell viability was evaluated by using

a CellTiter-Glo™ Luminescent Cell Viability Assay kit (Promega, Madison, WI, USA). Cell viability was calculated by comparing the number of viable cells incubated with SPIO samples over that from the cell medium control. The standard error was obtained from 3 replicate experiments.

MRI evaluation of SPIO uptake in cancer cells

H2009 lung cancer cells were grown in tissue culture flasks and incubated with LCP-SPIO or SP-SPIO nanoparticles at the Fe concentration of 0.03 mM for 0.5 and 2 h. After incubation, H2009 cells were washed with PBS three times, harvested by trypsinization and suspended in 100 μL 1% agarose gel. T_2-weighted images and T_2 relaxation times of cell suspensions were acquired on a Varian INOVA 4.7 T scanner. A spin echo sequence (TR = 5000 ms, TE = 45 and 60 ms, FOV = 35 × 35 mm, matrix = 128 × 128, slice thickness = 2 mm) was used for image acquisition.

Results

Surface modification and characterizations of SPIO nanoparticles

We chose to use the PEG-tethered Cys strategy to modify the surface of SPIO nanoparticles (Scheme 1). The thiol and carboxylate groups on Cys can form bi-dentate binding to the Fe ions on the SPIO surface.[21,22] Furthermore, oxidation of thiol groups can lead to crosslinked disulfide between Cys residues on the SPIO surface,[23–25] which can further increase the stability of ligand functionalization.

Fig. 1A demonstrates the success of SPIO surface modification strategy by the PEG-Cys method. The as-synthesized SPIO nanoparticles were coated with oleic acids at the surface and consequently very hydrophobic.[19] Partition of these SPIO nanoparticles between the hexane and aqueous phases (the top and bottom layers in Fig. 1A, respectively) shows that most of the particles stayed in the hexane phase (a in Fig. 1A). Treatment of as-synthesized SPIO nanoparticles with LCP peptide (NH_2-RGDLATLRQL-COOH) without the PEG-Cys group did not change the partition behavior of the SPIO nanoparticles (b in Fig. 1A). In comparison, surface treatment with PEG-Cys and LCP-PEG-Cys molecules resulted in complete partitioning of SPIO nanoparticles in the aqueous phase (c and d in Fig. 1A). When the –COOH group of Cys was replaced with $–CONH_2$, the resulting LCP-PEG_{11}-Cys-$CONH_2$ was not able to bind on the surface of SPIO particles through ligand exchange, and therefore failed to solubilize the SPIO particles in water under otherwise identical surface modification conditions (data not shown).

The attachment of PEG-Cys on the SPIO surface was further confirmed by the FTIR. As-synthesized SPIO nanoparticles have shown characteristic Fe–O vibration bands at 600 and 450 cm^{-1} (Fig. 1B).[26] In addition, surface-bound oleic acids can be observed by the presence of 2900 (C–H stretching) and 1620 (C=O stretching) cm^{-1} peaks. In the PEG-Cys modified SPIO sample, the Fe–O absorption bands were retained. Moreover, absorption peaks due to PEG-Cys (*e.g.*, 1100 and 1660 cm^{-1} peaks from PEG C–O–C and Cys C=O streching bands, respectively) were also observed. Based on the amino acid analysis of the peptides on the SPIO particles, we calculated that approximately 100–130 LCP(SP)-PEG-Cys chains were bound per 6 nm SPIO particle.

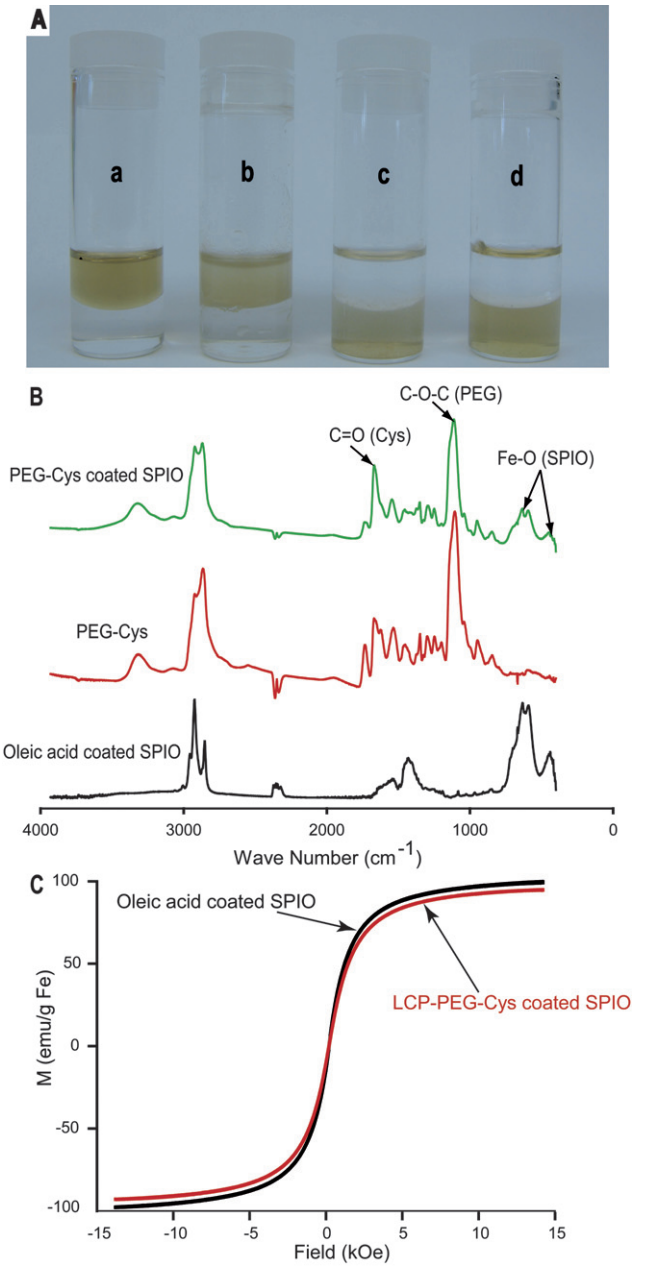

Fig. 1 (A) Solubility test of different surface modified SPIO particles dispersed in a water and hexane mixture (a) SPIO particles, (b) LCP treated SPIO particles, (c) PEG-Cys treated SPIO particles and (d) LCP-PEG-Cys treated SPIO particles; (B) FTIR spectra of oleic acid coated SPIO, free PEG-Cys and PEG-Cys coated SPIO; (C) Magnetic hysteresis loops of surface modified 6 nm SPIO particles.

The magnetic properties of the SPIO nanoparticles did not change significantly upon ligand exchange. Magnetic hysteresis data showed almost superimposable magnetization curves for the as-synthesized and LCP-PEG-Cys modified SPIO nanoparticles (Fig. 1C). The values of saturated magnetization moment (M_s) are approximately 90 emu/g Fe for both samples. This data suggests that ligand exchange on the surface of SPIO

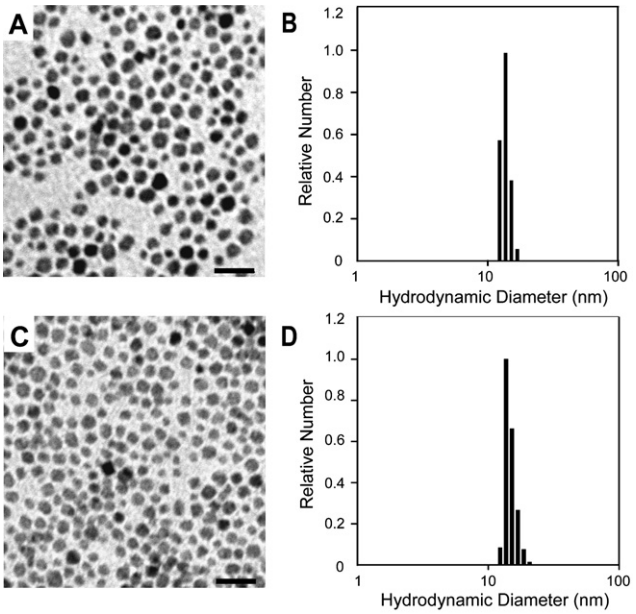

Fig. 2 TEM (A, C) and DLS (B, D) characterization of LCP/SP-PEG-Cys modified SPIO nanoparticles. (A, B) SPIO nanoparticles modified by LCP-PEG-Cys. (C, D) SPIO nanoparticles modified by SP-PEG-Cys. The scale bars in A and C are 20 nm.

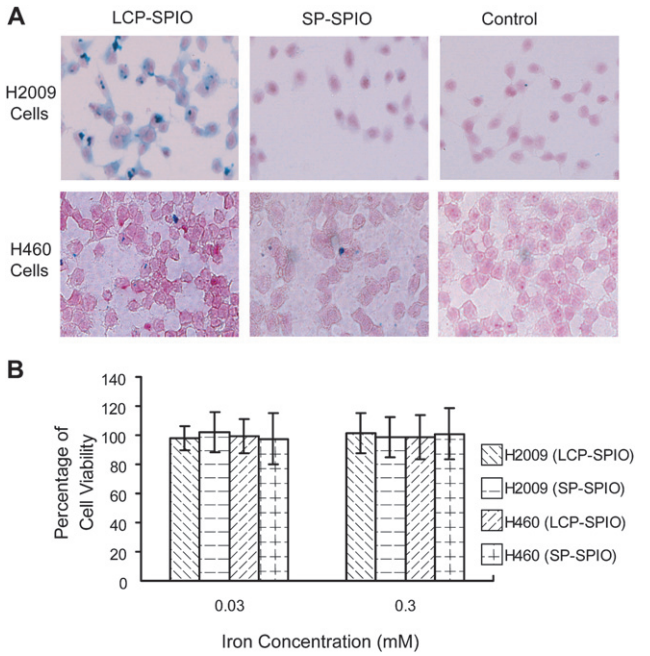

Fig. 3 Evaluation of cell targeting specificity and cytotoxicity of SPIO nanoprobes. (A) Prussian blue staining of $\alpha_v\beta_6$(+)-H2009 and $\alpha_v\beta_6$(−)-H460 cells treated with LCP-SPIO and SP-SPIO at 0.03 mM Fe concentration for 2 h; (B) percentage of cell viability after incubation with SPIO samples at Fe concentrations of 0.03 and 0.3 mM for 24 h.

did not considerably affect the SPIO nanocrystalline structure and magnetic properties.

The LCP/SP-PEG-Cys modified SPIO nanoparticles were further characterized by the TEM and DLS (Fig. 2). TEM data showed that both SPIO samples were singly dispersed on the copper grids without the formation of clustered SPIO aggregates. The average diameters were 6.2 ± 0.9 and 6.4 ± 1.1 nm for the LCP-SPIO and SP-SPIO, respectively. The DLS histograms (Fig. 2B and 2D) showed a single population of particle size distribution for both samples. The hydrodynamic diameters were 16.2 ± 2.5 and 15.7 ± 3.1 nm for the LCP-SPIO and SP-SPIO, respectively. The larger diameter from the DLS measurment reflects the contribution of the LCP/SP-PEG-Cys surface coatings (they are not visible under TEM) to the increase in hydrodynamic size.

Cell uptake and viability of LCP/SP-SPIO nanoparticles

To determine the targeting specificity of LCP-SPIO nanoparticles to $\alpha_v\beta_6$-positive lung cancer cells, we performed two experiments. In the first experiment, we compared the cell uptake efficiency of LCP-SPIO nanoparticles between $\alpha_v\beta_6$-positive H2009 and $\alpha_v\beta_6$-negative H460 cells. Prussian blue staining showed considerably increased Fe uptake in $\alpha_v\beta_6$-positive H2009 cells over $\alpha_v\beta_6$-negative H460 cells (Fig. 3A). Majority of the particles appear to be localized in the perinuclear region of the cell, consistent with the previous observation with LCP-modified quantum dots in H2009 cells.[18] In the second experiment, we compared the uptake efficiency in H2009 cells between the LCP-SPIO and SP-SPIO nanoparticles. Results show that cell targeting is peptide specific as the peptide with the scrambled sequence did not mediate significant SPIO uptake in H2009 cells. These results indicate that surface-bound LCP peptides maintained their biological activities and achieved cancer-specific targeting properties for the SPIO nanoprobes.

In order to evaluate whether peptide functionalization may induce toxicity to the cells, LCP-SPIO or SP-SPIO at two different Fe concentrations were incubated with H2009 or H460 cells for 24 h. Under these conditions, neither of the particles showed observable cytotoxicity (Fig. 3B).

Evaluation of SPIO targeting specificity to lung cancer cells by MRI

Prior to evaluation of SPIO targeting specificity to lung cancer cells, we examined and compared the MR relaxivities of the SPIO nanoparticles between LCP-SPIO and SP-SPIO. At 37 °C, both particle formulations showed similar MR relaxivities (Fig. 4A). More specifically, the T_1 and T_2 relaxivities were measured to be 11.5 and 142 s^{-1} Fe mM^{-1} for LCP-SPIO, respectively. In comparison, the T_1 and T_2 relaxivities were 12.1 and 141 s^{-1} Fe mM^{-1} for SP-SPIO, respectively. Thus, the particles show comparable intrinsic MR properties regardless of which peptide is conjugated at the surface.

MR imaging of H2009 cancer cells incubated with LCP-SPIO showed significantly reduced T_2 relaxation times over the SP-SPIO control (Fig. 4B). T_2 relaxation times were 27.3 ± 3.2 and 45.0 ± 5.2 ms after 0.5 h incubation for LCP-SPIO and SP-SPIO, respectively ($p = 0.05$). The difference is even more significant after 2 h incubation ($p = 0.01$), where T_2 relaxation times were 16.7 ± 2.5 and 35.6 ± 3.1 ms for LCP-SPIO and SP-SPIO, respectively. These results are consistent with the observation from the cell uptake studies (Fig. 3A), which demonstrates the $\alpha_v\beta_6$-targeting specificity of LCP-SPIO nanoprobes.

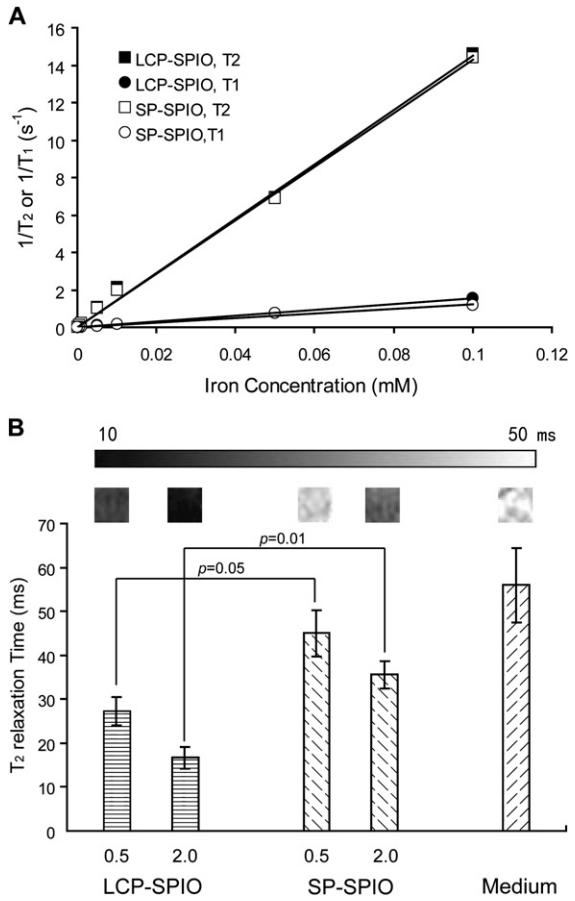

Fig. 4 Evaluation of cell targeting specificity of SPIO nanoprobes by MRI. (A) T_1 and T_2 relaxation rates as a function of Fe concentrations for LCP-SPIO and SP-SPIO; (B) T_2 relaxation times of H2009 cells treated with LCP-SPIO and SP-SPIO nanoprobes for 0.5 and 2 h. The *p* values were calculated by Student's *t*-test and showed statistical significance between the LCP-SPIO and SP-SPIO samples.

Discussion

Lung cancer is the leading cause of cancer-related deaths in the US and its five year survival rate is less than 15%.[2] When lung cancer is diagnosed early, surgical resection, radiation and chemotherapy can substantially improve survival. Currently, computed tomography (CT) and positron emission tomography (PET) are frequently used for lung tumor diagnosis.[27] These methods have shown limited accuracy (*e.g.* PET suffers from low spatial resolution)[28] and specificity (*e.g.* CT has high false positive rates[29]) for the diagnosis of lung cancer. The current study aims to develop highly specific SPIO nanoprobes and use the high spatial resolution capability of MRI for molecular diagnosis of lung cancer.

SPIO nanoparticles are the most commonly used T_2 contrast agents used in the clinics. Several different formulations (*e.g.* Feridex IV, Resovist) are clinically used for liver or GI tract imaging.[30] Most of these particles were synthesized by the low-temperature hydrolytic procedure that utilized alkaline precipitation of Fe^{2+}/Fe^{3+} salts. Their applications in cancer molecular imaging may be limited due to the high polydispersity of SPIO nanoparticles, low relaxation rates and lack of specificity *in vivo*. Recently, much attention has been devoted to the development of structurally well-defined superparamagnetic nanoparticles with high magnetization and MRI sensitivity.[31] High temperature nanocrystalization methods with $Fe(CO)_5$ or $Fe(acac)_3$ as precursors in the presence of surfactants (*e.g.* oleic acid) were established to yield SPIO nanoparticles with narrow size distributions.[19,32] In addition to Fe_3O_4, other SPIO compositions (*e.g.* $MnFe_2O_4$,[6] $Zn_xFe_{3-x}O_4$, $x < 0.5$[33]) have been synthesized with increased magnetization and T_2 relaxivity.

Our current surface functionalization strategy employs the use of monodisperse SPIO nanoparticles coated with hydrophobic surfactants. The proposed surface chemistry has several potential advantages. First, the procedure can lead to stably dispersed single SPIO particles in aqueous solution as demonstrated by the TEM and DLS. Because a defined PEG length of only 11 ethylene glycol units was used, the hydrodynamic size of the modified SPIO particles was narrowly distributed with only a few nanometres increase compared with inorganic Fe_3O_4 core. The relatively small hydrodynamic diameter (~16 nm) of the resulting SPIO nanoprobes may prove important in targeting lung cancer cells with enhanced tissue penetration properties. Second, after surface modification, the SPIO nanoparticles maintained its magnetic properties as demonstrated by the hysteresis curves (Fig. 1C). The direct conjugation strategy should also maintain the high intrinsic MR relaxivities of SPIO nanoparticles without possible attenuations by the introduction of a non-magnetic layer (*e.g.* SiO_2 or Au).[14,15] Third, the PEG-Cys design has resulted in stable ligand conjugation on the SPIO surface, which helped achieve the $\alpha_v\beta_6$-specific targeting of lung cancer cells. The bidentate chelation[21,22] and possible disulfide crosslinking[23–25] at the SPIO surface provide the thermodynamic driving force for the stable surface attachment of biological molecules. Similarly, Sun and coworkers have also utilized a bidentate strategy with 4-methylcatechol to achieve stable surface functionalization of SPIO particles.[5] Finally, our PEG-Cys design can be easily incorporated in a solid phase peptide synthesis protocol, which-can be generalized to a variety of small peptide molecules. This strategy provides a complementary approach to the use of amphiphilic micelle strategy for the solubilization and ligand modification of SPIO nanoprobes.[34–36] Further work is in progress to investigate the long-term stability of the surface coating, shelf-life and *in vivo* imaging efficacy of these SPIO nanoprobes.

Conclusions

In summary, we describe a facile chemical method to functionalize the surface of SPIO nanoparticles for molecular imaging of lung cancer. A lung cancer targeting peptide, H2009.1, was successfully introduced at the SPIO surface when a PEG-cysteine moiety was added to the carboxy-terminus of the peptide. The resulting SPIO nanoprobes demonstrated $\alpha_v\beta_6$-specific targeting of human H2009 lung cancer cells over the $\alpha_v\beta_6$-negative H460 control by Prussian blue staining and T_2-weighted MR imaging. The relatively small size, monodisperse size distribution, and versatile surface chemistry open up many opportunities for the implementation of biologically specific SPIO nanoprobes for molecular diagnosis of lung cancer.

Acknowledgements

This research is supported by the NIH grants R21EB005394 and R01CA129011 to JG, R01CA106646 and Welch (I1622) grants to KCB, and Lung Cancer SPORE P50CA70907 to JDM. GH is supported by a Susan G. Komen foundation postdoctoral fellowship (PDF0707216). CK is supported by a DOD Breast Cancer Research Program Multidisciplinary Postdoctoral Award (W81XWH-06-1-0751). SGY is partially supported by a Korean Research Foundation Grant (MOEHRD, KRF-2006-214-E00039). MR imaging was facilitated by the NCI SW-SAIR grant (U24 CA126608). This is CSCN045 from the program in Cell Stress and Cancer Nanomedicine, Simmons Comprehensive Cancer Center, UT Southwestern Medical Center.

References

1 WHO, *Cancer*, www.who.int, 2008.
2 A. Jemal, R. Siegel, E. Ward, Y. Hao, J. Xu, T. Murray and M. J. Thun, *CA Cancer J. Clin.*, 2008, **58**, 71–96.
3 Y. W. Jun, J. H. Lee and J. Cheon, *Angew. Chem., Int. Ed. Engl.*, 2008, **47**, 5122–5135.
4 S. Laurent, D. Forge, M. Port, A. Roch, C. Robic, L. Vander Elst and R. N. Muller, *Chem. Rev.*, 2008, **108**, 2064–2110.
5 J. Xie, K. Chen, H. Y. Lee, C. Xu, A. R. Hsu, S. Peng, X. Chen and S. Sun, *J. Am. Chem. Soc.*, 2008, **130**, 7542–7543.
6 J. H. Lee, Y. M. Huh, Y. W. Jun, J. W. Seo, J. T. Jang, H. T. Song, S. Kim, E. J. Cho, H. G. Yoon, J. S. Suh and J. Cheon, *Nat. Med.*, 2007, **13**, 95–99.
7 J. Park, G. Von Maltzahn, L. Zhang, M. P. Schwartz, E. Ruoslahti, S. N. Bhatia and M. J. Sailor, *Adv. Mater.*, 2008, **20**, 1630–1635.
8 N. Nasongkla, E. Bey, J. Ren, H. Ai, C. Khemtong, J. S. Guthi, S. F. Chin, A. D. Sherry, D. A. Boothman and J. Gao, *Nano Lett.*, 2006, **6**, 2427–2430.
9 V. Amirbekian, M. J. Lipinski, K. C. Briley-Saebo, S. Amirbekian, J. G. Aguinaldo, D. B. Weinreb, E. Vucic, J. C. Frias, F. Hyafil, V. Mani, E. A. Fisher and Z. A. Fayad, *Proc. Natl. Acad. Sci. U. S. A.*, 2007, **104**, 961–966.
10 C. Khemtong, C. W. Kessinger, J. Ren, E. Bey, S. Yang, J. S. Guthi, D. A. Boothman, A. D. Sherry and J. Gao, *Cancer Res.*, 2009, **69**, 1651–1658.
11 D. Hogemann-Savellano, E. Bos, C. Blondet, F. Sato, T. Abe, L. Josephson, R. Weissleder, J. Gaudet, D. Sgroi, P. J. Peters and J. P. Basilion, *Neoplasia*, 2003, **5**, 495–506.
12 F. Sonvico, S. Mornet, S. Vasseur, C. Dubernet, D. Jaillard, J. Degrouard, J. Hoebeke, E. Duguet, P. Colombo and P. Couvreur, *Bioconjug. Chem.*, 2005, **16**, 1181–1188.
13 D. Artemov, N. Mori, B. Okollie and Z. M. Bhujwalla, *Magn. Reson. Med.*, 2003, **49**, 403–408.
14 J. Lee, Y. Lee, J. K. Youn, H. B. Na, T. Yu, H. Kim, S. M. Lee, Y. M. Koo, J. H. Kwak, H. G. Park, H. N. Chang, M. Hwang, J. G. Park, J. Kim and T. Hyeon, *Small*, 2008, **4**, 143–152.
15 M. Mandal, S. Kundu, S. K. Ghosh, S. Panigrahi, T. K. Sau, S. M. Yusuf and T. Pal, *J. Colloid Interface Sci.*, 2005, **286**, 187–194.
16 H. Guan, M. J. McGuire, S. Li and K. C. Brown, *Bioconjug. Chem.*, 2008, **19**, 1813–1821.
17 T. Oyama, K. F. Sykes, K. N. Samli, J. D. Minna, S. A. Johnston and K. C. Brown, *Cancer Lett.*, 2003, **202**, 219–230.
18 A. N. Elayadi, K. N. Samli, L. Prudkin, Y. H. Liu, A. Bian, X. J. Xie, Wistuba, II, J. A. Roth, M. J. McGuire and K. C. Brown, *Cancer Res.*, 2007, **67**, 5889–5895.
19 S. Sun, H. Zeng, D. B. Robinson, S. Raoux, P. M. Rice, S. X. Wang and G. Li, *J. Am. Chem. Soc.*, 2004, **126**, 273–279.
20 R. M. Phelps, B. E. Johnson, D. C. Ihde, A. F. Gazdar, D. P. Carbone, P. R. McClintock, R. I. Linnoila, M. J. Matthews, P. A. Bunn, Jr., D. Carney, J. D. Minna and J. L. Mulshine, *J. Cell Biochem. Suppl.*, 1996, **24**, 32–91.
21 H. Handa, M. Abe and M. Hasegawa, *US Pat.*, 20050084539, 2005.
22 E. B. Borghi, P. J. Morando and M. A. Blesa, *Langmuir*, 1991, **7**, 1652–1659.
23 K. Nishio, N. Gokon, S. Tsubouchi, M. Ikeda, H. Narimatsu, S. Sakamoto, Y. Izumi, M. Abe and H. Handa, *Chem. Lett.*, 2006, **35**, 974–975.
24 A. Amirbahman, L. Sigg and U. Gunten, *J. Colloid Interface Sci.*, 1997, **194**, 194–206.
25 N. Fauconnier, J. N. Pons, J. Roger and A. Bee, *J. Colloid Interface Sci.*, 1997, **194**, 427–433.
26 M. Ma, Y. Zhang, W. Yu, H. Y. Shen, H. Q. Zhang and N. Gu, *Colloids Surf., A*, 2003, **212**, 219–226.
27 M. M. Oken, P. M. Marcus, P. Hu, T. M. Beck, W. Hocking, P. A. Kvale, J. Cordes, T. L. Riley, S. D. Winslow, S. Peace, D. L. Levin, P. C. Prorok and J. K. Gohagan, *J. Natl. Cancer Inst.*, 2005, **97**, 1832–1839.
28 D. W. Townsend, *Ann. Acad. Med. Singapore*, 2004, **33**, 133–145.
29 E. M. Toloza, L. Harpole and D. C. McCrory, *Chest*, 2003, **123**, 137S–146S.
30 Y. X. J. Wang, S. M. Hussain and G. P. Krestin, *Eur. Radiol.*, 2001, **11**, 2319–2331.
31 J. Park, J. Joo, S. G. Kwon, Y. Jang and T. Hyeon, *Angew. Chem., Int. Ed. Engl.*, 2007, **46**, 4630–4660.
32 T. Hyeon, S. S. Lee, J. Park, Y. Chung and H. B. Na, *J. Am. Chem. Soc.*, 2001, **123**, 12798–12801.
33 C. Barcena, A. K. Sra, G. S. Chaubey, C. Khemtong, J. P. Liu and J. Gao, *Chem. Commun.*, 2008, 2224–2226.
34 H. Ai, C. Flask, B. Weinberg, X. Shuai, M. D. Pagel, D. Farrell, J. Duerk and J. Gao, *Adv. Mater.*, 2005, **17**, 1949–1952.
35 W. W. Yu, E. Chang, C. M. Sayes, R. Drezek and V. L. Colvin, *Nanotechnology*, 2006, **17**, 4483–4487.
36 N. Nitin, L. E. LaConte, O. Zurkiya, X. Hu and G. Bao, *J. Biol. Inorg. Chem.*, 2004, **9**, 706–712.

